Annals of Hematology (2019) 98:595–603
https://doi.org/10.1007/s00277-019-03608-y

ORIGINAL ARTICLE

Detection of AML-specific mutations in pediatric patient plasma using extracellular vesicle–derived RNA

Fabienne Kunz[1] · Evangelia Kontopoulou[1] · Katarina Reinhardt[1] · Maren Soldierer[1] · Sarah Strachan[1] · Dirk Reinhardt[1] · Basant Kumar Thakur[1]

Received: 23 November 2018 / Accepted: 4 January 2019 / Published online: 23 January 2019

Abstract

Despite high remission rates, almost 25% of patients with AML will suffer relapse 3–5 years after diagnosis. Therefore, in addition to existing diagnostic and MRD detection tools, there is still a need for the development of novel approaches that can provide information on the state of the disease. Extracellular vesicles (EVs), containing genetic material reflecting the status of the parental cell, have gained interest in recent years as potential diagnostic biomarkers in cancer. Therefore, isolation and characterization of blood and bone marrow plasma-derived EVs from pediatric AML patients could be an additional approach in AML diagnostics and disease monitoring. In this study, we attempt to establish a plasma EV-RNA-based method to detect leukemia-specific FLT3-ITD and NPM1 mutations using established leukemia cell lines and primary pediatric AML plasma samples. We were successfully able to detect FLT3-ITD and NPM1 mutations in the EV-RNA using GeneScan-based fragment-length analysis and real-time PCR assays, respectively, in samples before therapy. This was corresponding to the gDNA mutational analysis from leukemic blasts, and supports the potential of using EV-RNA as a diagnostic biomarker in pediatric AML.

Keywords Extracellular vesicles · RNA · Pediatric AML · Biomarker

Introduction

Acute myeloid leukemia (AML) is a very heterogeneous hematological cancer and is the second most common form of leukemia in children [1]. Although there is a high remission rate for AML patients (up to 80%), relapse continues to be the most common cause of death in AML [2, 3]. One of the major challenges in predicting relapse in AML lies in the acquisition of novel secondary mutations in the primary leukemic cells during therapy [1, 4]. Additionally, there is lack of an effective uniform molecular biomarker which can monitor clonal evolution to predict minimal residual disease and relapse [2, 3, 5]. Although cellular analysis of blasts can be effective for diagnosis, the presence of them in the blood can reflect that the disease has already reached an advanced level; therefore, there is a strong need for an alternative diagnostic tool which can predict relapse at an earlier time point.

Extracellular vesicles (EVs) have recently gained interest in the field of cancer due to their novel roles as biomarkers and cell to cell mediators in metastasis and relapse [6, 7]. EVs are a mixed group of membrane-bound vesicles, with exosomes and microvesicles being the two main subtypes of interest in research [8–10]. They are produced by both healthy and cancerous cells and can be found in several body fluids, like blood, urine, or saliva, from where they can be easily isolated and analyzed using a simple liquid biopsy approach [6]. Additionally, it has been shown that the nucleic acids found within EVs can potentially mirror the mutational status of the parental cell from which the EVs originate [6, 11], making them potential candidates for the development of diagnostic tools that could be utilized in a clinical setting.

Furthermore, several other working groups have previously demonstrated that EVs and the RNA they contain have

Fabienne Kunz and Evangelia Kontopoulou contributed equally to this work.

Electronic supplementary material The online version of this article (https://doi.org/10.1007/s00277-019-03608-y) contains supplementary material, which is available to authorized users.

✉ Basant Kumar Thakur
Basant-Kumar.Thakur@uk-essen.de

[1] Department of Pediatric Hematology and Oncology, University Hospital Essen, Hufelandstraße 55, D-45147 Essen, Germany

several characteristics, which could make them ideal biomarkers for the AML disease state. For example, earlier studies have claimed that cancerous cells produce more EVs than healthy cells [6, 12], which has also been observed in the AML disease state, with AML patients having higher numbers of EVs in circulation than healthy controls [13–15]. It has also been shown that the contents of EVs from AML cells can change depending on the disease stage [13], including the upregulation of several miRNAs that are relevant to AML prognosis and relapse [13, 16]. This is further supported by the previous work of Hornick et al. (2015) who showed that EV miRNA could be used to detect leukemic relapse in a mouse model [2, 5]. Furthermore, Huan et al. (2013) have previously shown that it is possible to detect AML-specific mRNA transcripts in EVs from conditioned media of cultured primary leukemia cells and AML cell lines [17] and, in addition, Hong et al. (2014) have previously shown that the level of TGF-β1 protein in EVs can be correlated to the status of therapy in AML [18]. All of these findings further support the idea of using EVs and their RNA content for the detection and monitoring of AML [2, 5, 17, 18].

In this study, for the first time, EV-RNA from primary pediatric patient plasma was investigated for its diagnostic value by attempting to detect AML-specific mutations in the EV-RNA at time points of diagnosis and during treatment. The plasma EV-based method to detect leukemia cell–specific information could potentially provide complimentary data on the stage of leukemia, disease progression, and response to therapy. In future, this could offer an alternative or additional tool to the classical bone marrow puncture for the detection and prediction of pediatric AML.

Material and methods

Ultracentrifugation of patient samples

Seventy-three plasma samples from 16 patients with childhood AML were obtained from the biobank of the Children's Hospital of Essen. Plasma from patients was obtained in varying volumes; therefore, before performing differential centrifugation and ultracentrifugation steps for EV isolation, the sample volume was adjusted to 2 ml by adding PBS, as required. A normal centrifugation for 20 min at 3000×*g* at 10 °C had been previously performed. The supernatant was collected in new tubes and centrifuged at 12,000×*g* for 20 min at 10 °C. The supernatant was transferred into 4-ml ultracentrifuge tubes (Beckman Coulter No. 355645) and samples were balanced with a maximum difference of 0.01 g before performing ultracentrifugation. Samples were ultracentrifuged using a fixed angle rotor Ti 50.4 (Beckman Coulter) at 100,000×*g* for 70 min at 10 °C. The supernatants were discarded and the pellet containing EVs was washed by resuspending in 2 ml of PBS and ultracentrifuged at 100,000×*g* for 70 min at 10 °C. After discarding the supernatant, the final EV pellet was resuspended in 250 μl of PBS. From the obtained EV pellet, 20 μl was used as aliquots for further analysis.

The same protocol was used for the isolation of EVs from conditioned media of leukemia cell lines, with the only differences being the volume and the rotor (Ti 45, Beckman Coulter) which were used. The conditioned media from each flask of each leukemia cell line were transferred into one 94-ml ultracentrifuge tube (Beckman Coulter No. 355628) and was ultracentrifuged to obtain purified EVs. The final EV pellets were resuspended in 250 μl of PBS, transferred into microcentrifuge tubes, and frozen at − 80 °C.

Cell culture

Leukemia cell line MV4-11 (acute monocytic leukemia) was cultured in RPMI-1640 media (Gibco No. 21875-034) with 10% FBS (Biowest, No. S1860-500) and 1% Pen-Strep (Gibco No. 15140-122), and OCI-AML3 (acute myeloid leukemia) was cultured in MEM Alpha media (Gibco No. 12561056) with 20% FBS and 1% Pen-Strep . When enough cells were obtained, the cells from each flask were centrifuged at 300×*g* for 5 min and the pellet was resuspended in 1 ml of RPMI-1640 media or MEM Alpha media with 10% or 20% EV-depleted FBS and 1% Pen-Strep. Next, 3.5×10^6 cells were then transferred into 12 T175 flasks (Cell star No. 660175) with 24 ml of EV-depleted media. This assured that the supernatant would contain only EVs released from the cells. After 48 h, an additional 25 ml of this media was added to the flasks and left for an additional 24 h. This supernatant was collected and used in ultracentrifugation to obtain EVs for further analysis.

ZetaView analysis—nanoparticle tracking analysis

Nanoparticle tracking analysis (NTA-ZetaView, Particle Metrix GmbH) was performed to characterize EVs according to the recommendations of the International Society of Extracellular Vesicles (ISEV). Fresh standards were prepared using "100 nm standard beads." First, 10 μl of standard was added to 10 ml of H_20 (1:1000). Then, 188 μl of the 1:1000 solution was transferred into another falcon which contained 50 ml H_20 (1:266,000). All the settings were adjusted using the standard beads, and the concentration of the samples was adjusted using DPBS in order to obtain the number and the size of the particles that did not exert the minimum and maximum values of the settings. The final volume of diluted samples loaded onto the ZetaView was 1 ml. At least two washes of 10 ml DPBS were performed to clean the sample loading platform of the ZetaView between the measurements of each sample. The zeta potential, number of EVs, and size histograms were generated by built-in software of the ZetaView instrument.

RNA isolation and quantification

The RNA isolation was performed using the NucleoSpin® RNA XS (Macherey-Nagel No. 740902.50) according to the manufacturer's instructions. Briefly, 200 μl of Buffer RA1 and 4 μl of TCEP were added to each 50 μl isolated EV sample and vortexed vigorously. Next, 300 μl of 70% ethanol was added to the homogenized lysate and mixed by pipetting. Each sample was loaded into a Nucleospin RNA XS column and centrifuged at 11,000×*g* for 30 s. Then, 100 μl MDB (Membrane Desalting Buffer) was added and centrifuged at 11,000×*g* for 30 s. Next, 25 μl of rDNase reaction mixture was applied directly onto the center of the column and incubated at RT for 15 min. A wash step was performed by adding 100 μl of Buffer RA2 to the column, followed by a centrifugation of 11,000×*g* for 30 s. Two extra washing steps took place by applying 400 μl and 200 μl of Buffer RA3 and centrifuged at 11,000×*g* for 30 s and 2 min, respectively. RNA was eluted in 45 μl of RNase-free H_2O. The RNA concentration was quantified using the RNA Quantifluor (Promega No. E3310) system according to the instructions of the manufacturer.

cDNA synthesis

The isolated RNA was transcribed into cDNA using a Transcriptor First Strand DNA Synthesis Kit (Roche No. 04897030001). Briefly, 2 μl of the provided random hexamer primer and 11 μl of RNA were transferred into a 0.2-ml Eppendorf tube. The samples were heated for 10 min at 65 °C and then cooled on ice. Next, 7 μl of a master mix consisting of the provided reverse transcriptase reaction buffer, protector RNase inhibitor, deoxynucleotide mix, and reverse transcriptase was added to the RNA/oligonucleotide primer solution, to a final volume of 20 μl. For the cDNA synthesis, samples were heated at 25 °C for 10 min, followed by 55 °C for 30 min and 85 °C for 5 min in a C1000 Thermal Cycler (Bio-Rad).

GeneScan-based fragment-length analysis

For the detection of the FLT3-ITD mutation, GeneScan-based fragment-length analysis was performed. First, PCR was performed with the following primers: FLT3-ITD forward 5′-GTAAAACGACGGCCAGGCAATTTAGGTATGAAAGCCAGC-3′ and reverse 5′-CAGGAAACAGCTATGACCTTTCAGCATTTTGACGGCAACC-3′ (Eurofins). Next, 20.5 μl of the Master Mix (which contained 12.5 μl ALL in Hot Start Taq 2× MM (HighQu), 6 μl H_2O, and 1 μl of the forward and reverse primers with a concentration of 10 pmol/μl) was added together with 4.5 μl of the sample into a 0.5-ml Eppendorf tube. The same mixture without the sample was prepared as control. For amplification, samples were heated at 95 °C for 2 min, followed by 40 cycles of 95 °C for 15 sec, 59 °C for 15 sec, and 72 °C for 15 sec. PCR products were diluted (1:80) in H_2O. Next, 1 μl of diluted PCR products was mixed with 10 μl HiDi Formamid (Thermo Fisher) and 0.3 μl GeneScan-based fragment-length analysis 600 LIZ Size Standard v 2.0 (Thermo Fisher). PCR products were denatured for 5 min at 95 °C. GeneScan-based fragment-length analysis was performed using the 3500 genetic analyzer and data were analyzed with GeneMapper Software 5 (Thermo Fisher).

RT-PCR

Qualitative and quantitative detection of the mutated NPM1 gene (OMIM No. 1640401) was done by RT-PCR. The protocol has been optimized from the standard operational procedure (SOP), which was developed by the European molecular net. The following primers were used: NPM1_forward: 5′-CAAAGTGGAAGCCAAATTCATC-3′; NPM1_reverse: 5′-CCTCCACTGCCAGACAGA-3′; probe: 5′-TAGC CTCTTGGTCAG-TCATCCGGAAGCA [BHQ1]-3′ (Eurofins). The ABL2 gene (OMIM 164690) was used as a housekeeping gene: ABL_forward: 5′-GGGT CCACACTGCAATGTTT-3′; ABL_reverse: 5′-CCAA CGAGCGGCTTCAC-3′; probe: 5′-TCAGATGCTACTGG CCGCTGAAGG [BHQ1]-3′. Probes were synthesized by Eurofins (Ebersberg). All samples were performed in triplicate, including controls (ABL2 and H_2O). In each well of a 96-well plate, 17 μl of the Master Mix, 12.5 μl of TaqMan Universal Master Mix (Thermo Fisher), 2 μl of H_2O, and 2.5 μl of 10× primer mix were added. This primer mix contained 3 μM of the primer (forward/reverse) and 2 μM of the probe (FAM and H_2O). Next, 3 μl of cDNA was added to each well, which was then sealed with optical caps. The plate was briefly spun down and loaded onto the StepOne™ Real-Time PCR System (Thermo Fisher).

Transmission electron microscopy

Transmission electron microscopy (TEM) was performed at the Imaging Center Essen (IMCES) for visualization of the EVs. Firstly, mesh copper grids coated with formvar (PLANO No. SF162) were made hydrophilic by exposing them to glow discharging for 1.5 min (PELCO easiGlow™). Afterwards, 3 μl of EV sample was added to the grids, which were then negatively stained for 1 min with 3 μl of 1% *v/v* uranyl acetate. The excess liquid was removed and the grids were dried for 15 min and finally observed under a JEOL 1400+ TEM Crossbeam at 120 kV (JEOL).

Results

EV isolation from leukemia cell lines

Two different cell lines, OCI-AML3 carrying a NPM1 mutation and MV4-11 carrying a FLT3-ITD mutation, were cultured for 72 h in EV-depleted growth medium. EVs were extracted from conditioned medium using differential centrifugation followed by ultracentrifugation steps. The characterization of the EVs (Supplementary Table S1), to estimate their number and their average diameter, was performed by NTA. Average particle size of both cell lines was in the range of 30–160 nm (Fig. 1a, b, Supplementary Fig. 1a). Transmission electron microscopy was performed to visualize EVs in order to further confirm their presence and size (Fig. 1b–e). These results confirmed the successful isolation of EVs based on the expected EV size range (30–150 nm), allowing the continuation of further molecular analyses.

EV-derived RNA from leukemia cell lines reflects the genomic mutational status

To firstly check whether it was possible to detect the mutations in each cell line and to compare the mutational status of the cell lines with their EVs, RNA was extracted from the EVs (Fig. 2a) and cells of both cell lines. The RNA was transcribed into cDNA and the mutational detection was performed by two different assays. RT-PCR was used for the detection of the NPM1 mutation, while GeneScan-based fragment-length analysis was performed for the FLT3-ITD mutation. The NPM1 mutation was detectable in RNA extracted from both cells and EVs (Fig. 2b, Supplementary Fig. 1b and c). The FLT3-ITD mutation was also

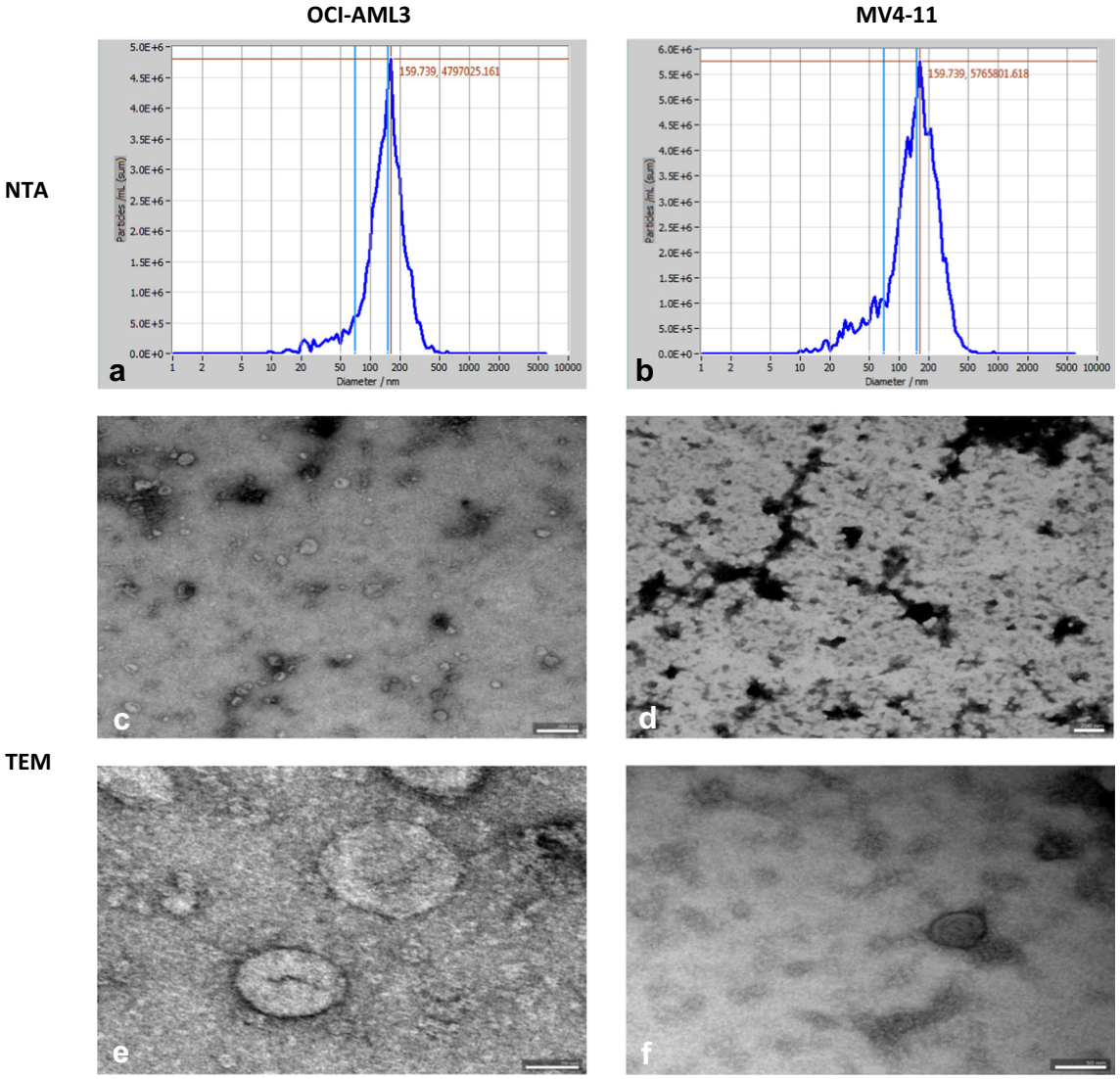

Fig. 1 **a**, **b** Particle diameter size and number of particles in leukemia cell line supernatant, as measured by nanoparticle tracking analysis (NTA). The size distribution is in the range of extracellular vesicles (30–160 nm). **c**–**f** Transmission electron microscopy of uranyl acetate–stained EVs from leukemia cell line supernatant. Scale bar 200 nm

a

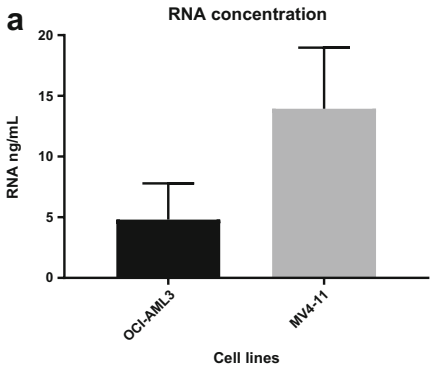

b

Cell line	NPM1	FLT3-ITD
OCI-AML3 EVs	+	-
OCI-AML3 cells	+	-
MV4-11 EVs	-	+
MV4-11 cells	-	+

Fig. 2 **a** Comparison of RNA concentration, extracted from EVs of two leukemia cell lines. **b** Results of RNA mutational analyses. RT-PCR analyses for NPM1 mutation were performed to compare the sensitivity of mutational detection in RNA that was extracted from EVs of one cell line (OCI-AML3) with the RNA extracted from the cells of both cell lines. For the assay, maximum volume of 3 μl was used from each sample. The NPM1 AML-specific mutations were not present in negative control cell line (MV4-11), however, the OCI-AML3 cell RNA and EV-RNA were both positive for the NPM1 mutation. GeneScan-based fragment-length analyses for detection of FLT3-ITD mutation in MV4-11 cell RNA and EV RNA were also performed. Negative control OCI-AML3 cell RNA was negative for the FLT3-ITD mutation and MV4-11 cell RNA and EV-RNA were positive for the FLT3-ITD mutation

detectable in both cases and, interestingly, was higher expressed in EVs in comparison with cell-derived RNA (Fig. 2b).

EV isolation from pediatric AML patient samples

To further investigate if the mutational status of a patient can be detected from plasma-derived EVs, EVs were isolated from AML patient samples by performing differential centrifugation followed by ultracentrifugation steps. The plasma-derived EVs were analyzed for their number and size by NTA, and the number of EVs obtained from samples before and after treatment was compared (Supplementary Tables S2 and S3). The average particle size was in the range of 30–160 nm (Fig. 3a–d) and TEM was performed to confirm the NTA results (Fig. 3e–h). In patients carrying the NPM1 mutation, as well as in patients with a combined mutation (NPM1 and FLT3-ITD), the number of particles was always lower in the after-treatment EV samples than in the before-treatment EV samples (Fig. 3i). In contrast, the patient group with the FLT3-ITD mutation only revealed a higher particle concentration in the after-treatment samples compared with the before-treatment samples (Fig. 3i). A decrease in the number of EVs after treatment would be expected as this would correlate with the decrease in cancerous cells, as well as with the reduced leukemic blast cells after treatment (Supplementary Table S2). The number of the EVs in the before-treatment samples between the different mutational groups is statistically significantly different revealing a correlation between the number of the released EVs and the mutational group that they belong to.

EV samples from pediatric AML patients contain RNA

To establish the EV-RNA as a potential tool for the detection of AML mutations in patient samples, RNA was extracted from the plasma-derived EVs of 16 AML patients. The EV-RNA concentration was measured by RNA QuantiFluor (Supplementary Table S3). The amount of obtained EV-derived RNA was higher in the before-treatment samples than in the after-treatment samples in AML patients with the NPM1 mutation only or with a combined mutation (Fig. 4a). In contrast, the EV-derived RNA from patients with the FLT3-ITD mutation only showed higher concentrations after treatment in comparison with the before-treatment samples (Fig. 4a). This mirrors the results of the NTA, which indicate the same trend in EV number.

EV-derived RNA reflects the patient mutational status

Next, we investigated whether the EV-RNA of the AML patients reflected their mutational status. EV-RNA from patients carrying a NPM1 mutation was obtained, transcribed into cDNA, and analyzed for the mutational status by RT-PCR. In seven AML patients, identical mutations were detected in the EV-RNA of the initial samples before therapy and in the primary leukemic blasts. In two patients, it was not possible to detect the mutation in the initial sample at all (Fig. 4b, Supplementary Table S4). In all patient samples after therapy, the initial AML-specific mutation was no longer detectable (Fig. 4b, Supplementary Table S4). GeneScan-based fragment-length analysis was performed for the mutational analysis of nine AML patients with a FLT3-ITD mutation. For this purpose, EV-derived RNA was extracted and transcribed into cDNA and GeneScan-based fragment-length analysis was performed. The mutation was detectable in all of the initial samples before treatment (Fig. 5a–d), but it was not possible to detect it in the after-treatment samples of each patient (Supplementary Table 4). This lack of mutational detection for both mutations in all after-treatment patient samples was not always in correlation to the results of the gDNA analysis that is routinely performed in our diagnostic AML lab after every treatment.

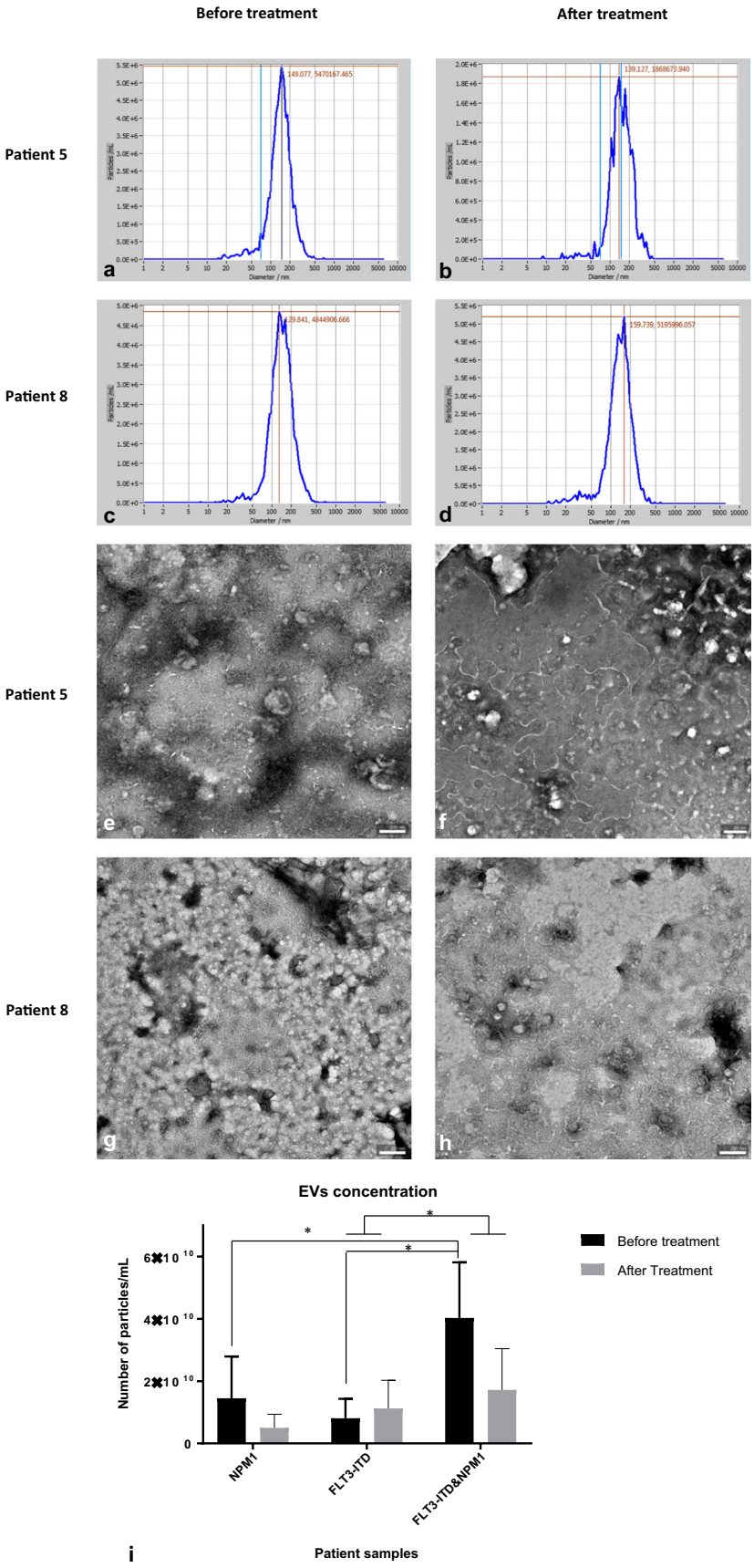

Fig. 3 **a**–**d** Particle diameter size and number of particles per mL of plasma from two AML patients before and after treatment, as measured by nanoparticle tracking analysis (NTA). The size distribution is in the range of extracellular vesicles (30–160 nm). **e**–**h** Transmission electron microscopy of uranyl acetate–stained EVs from patient plasma samples before and after treatment. Scale bar 200 nm. **i** Comparison of EVs concentration in before- and after-treatment samples from 16 AML patients, as measured by NTA analysis. Higher concentration of EVs in before-treatment samples was observed in patients with NPM1 mutation only and with combined mutations than those with a FLT3-ITD mutation only. The difference in EV concentration between patients with a FLT3-ITD mutation only and patients with FLT3-ITD and NPM1 combined mutations was statistically significant ($p = 0.0145$). In addition, EV concentration in before-treatment samples of patients carrying both mutations was statistically significantly higher than in the NPM1 only group ($p = 0.0468$) and the FLT3-ITD only group ($p = 0.0168$)

Discussion

Despite the recent advances in the treatment and diagnosis of AML, which is reflected by high remission rates, many patients are still suffering from relapse—the biggest cause of death in AML [2, 3]. This highlights the ongoing need for the development of a more sensitive approach with the ability to detect and monitor this disease more effectively. Simultaneously, this approach should encompass the advantage of reducing pain and inconvenience for the patients caused by the current standard bone marrow puncture–based diagnostic methods. In the current study, we attempted to take the first steps towards the development of a tool that would fulfill these criteria by evaluating the diagnostic potential of plasma-derived EV-RNA in pediatric AML.

Here, using both established leukemia cell lines and AML pediatric patient samples ($n = 16$), we have demonstrated the biomarker potential of EV-derived RNA in AML. Using cell line–conditioned media, we successfully established that it was possible to isolate EVs, extract RNA, and detect AML-specific mutations, NPM1 and FLT3-ITD, using RT-PCR and GeneScan-based fragment-length analysis methods, respectfully. These positive results reflected that our proposed isolation and detection methods were valid and functional at the cell line level. Subsequently, using the same methods, RNA was isolated from EVs of pediatric patient plasma ($n = 16$), before and after treatment, and analyzed for its biomarker potential. In 14 out of the 16 AML patient samples at the stage of primary diagnosis, it was possible to detect NPM1 or FLT3-ITD mutations which reflected the known gDNA information of the samples. These initial results showed that our approach was sensitive enough to detect AML-specific mutations from a source of plasma containing heterogeneous populations of EVs, highlighting that the approach does indeed have

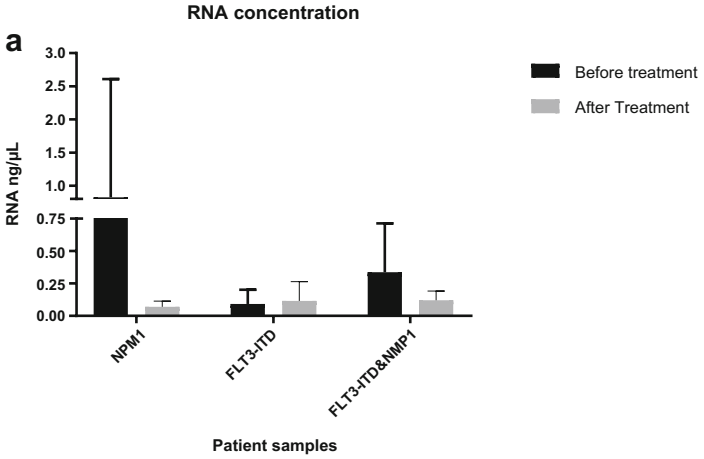

b

Patient	Mutation	Primary leukemia blasts	EV RNA Before treatment	EV RNA After treatment in different blocks						
P3	NPM1	+	+	-*	-*	-*	-*			
P4	NPM1	+	+	-	-	-	-	-		
P5	NPM1	+	+	-			-			
P7	NPM1	+	+	-*	-*	-*	-*	-*	-	-
P9	NPM1	+	+	n.a						
P10	NPM1	+	+	-*	-*	-*	-*			
P14	NPM1	+	+	-		-*				
P15	NPM1	+	n.a	-*		-*				
P16	NPM1	+	n.a	-*		-*				

Fig. 4 **a** Comparison of RNA concentration, extracted from EV fractions of 16 AML patients, prior and post treatment. **b** RT-PCR for NPM1 mutation was performed to establish the sensitivity of mutational detection in RNA that was extracted from EVs of patients, and compared with the already existing patient mutational status information of the primary leukemia database in the AML-BFM lab. Sixteen patient samples before and after treatment were used for analysis. A maximum volume of 3 µl from each sample was used. AML-specific mutations were not present in post-treatment samples.*Low-quality sequencing data. -*No mutation detected but low-quality sequencing data

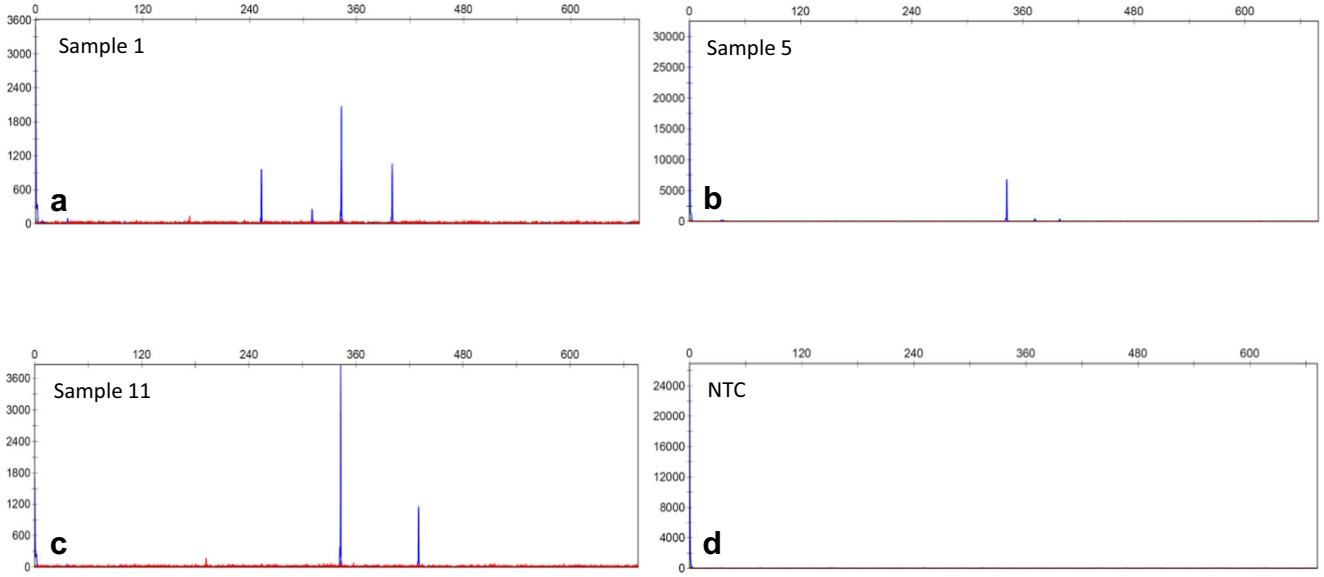

Fig. 5 **a**–**d** GeneScan-based fragment-length analysis of FLT3-ITD mutation was performed to establish the sensitivity of mutational detection in RNA that was extracted from EVs of patient samples, and compared with the already existing patient mutational status information of the primary leukemia database in the AML-BFM lab. Sixteen patient samples before and after treatment were used for analysis. 50 ng/μl or a maximum volume of 10.5 μl from each sample was used. Samples **a**, **b**, and **c** are before-treatment samples that show the FLT3-ITD mutation (size ~ 372). Sample **d** is the negative control. AML-specific mutations were not present in post-treatment samples (data not shown)

diagnostic biomarker potential. In addition, the number of EVs and the consequent amounts of RNA appeared to be influenced by the mutational background of the patients. As previous studies have shown that AML patients have more EVs than healthy controls [13–15], this was an interesting observation, which once established in a larger patient cohort study may have additional diagnostic utility.

The proposed approach, with the current sensitivity, does in fact have its limitations. Although it was successful at detecting mutations in almost all patients at initial diagnosis, it was not always possible to detect mutations after treatment when using this method. These are issues that must be addressed, as sensitivity is of utmost importance when designing diagnostic detection methods. These results could be attributed to the lower amount of RNA that was recovered from these samples; perhaps due to a reduction in EV production by mutation-containing cells or a reduction of the cells themselves. Alternatively, they could also be related to the EV heterogeneity of the plasma. Like all new approaches, this method also requires a period of optimization before its implementation as a clinically routine method can be considered. Therefore, in future, this study should be repeated using a larger cohort of patients and with an enhanced EV isolation method, capable of specifically sorting for AML-derived EVs.

Despite the discussed points of needed improvements in sensitivity, the advantage of this method over current diagnostic methods is clear, in terms of patient welfare. A liquid biopsy approach could indeed be a valuable diagnostic tool, offering a fast, pain-free, and hassle-free alternative to current painful bone marrow biopsies. Being able to diagnose or monitor a leukemic disease simply by drawing blood and isolating EVs instead of having to undergo a bone marrow puncture procedure would be much more convenient and less stressful for pediatric patients. In conclusion, our approach to establish an EV-RNA-based diagnostic platform provides valuable information that could be potentially useful in the future diagnosis and treatment of AML. This preliminary study definitely provides a starting point for the use of EV-RNA as a disease biomarker in AML and, once the sensitivity is optimized and the study is recapitulated in larger cohorts of patients, will open the door to many possible avenues of future research on this topic.

Authors' contributions Conception and design: BKT, FK, EK; collection and assembly of data: FK, EK, KR, MS; data analysis and interpretation: BKT, FK, EK; drafting of manuscript: BKT, FK, EK, SS; manuscript writing: BKT, FK, EK, SS; final approval of manuscript: all co-authors.

Funding This study was supported by the José Carreras Leukemia Foundation promotion grant 04 PSG/2017 awarded to Fabienne Kunz and Stiftung Universitätsmedizin Essen grant on cancer exosome research awarded to Dr. Basant Kumar Thakur.

Compliance with ethical standards

Conflict of interest The authors declare that they have no conflict of interest.

Informed consent Informed consent was obtained from all individual participants (or their parents) included in the study. Each patient consented following institutional review board approval AML-BFM 2004 (3VCreutzig1).

Ethical approval All procedures performed in studies involving human participants were in accordance with the ethical standards of the institutional and/or national research committee and with the 1964 Helsinki declaration and its later amendments or comparable ethical standards.

Statement on the welfare of animals This article does not contain any studies with animals performed by any of the authors.

Publisher's Note Springer Nature remains neutral with regard to jurisdictional claims in published maps and institutional affiliations.

References

1. Trino S, Lamorte D, Caivano A, Laurenzana I, Tagliaferri D, Falco G, Del Vecchio L, Musto P, and De Luca L (2018) MicroRNAs as new biomarkers for diagnosis and prognosis, and as potential therapeutic targets in acute myeloid leukemia, Int J Mol Sci 19(2):460
2. Hornick NI, Huan J, Doron B, Goloviznina NA, Lapidus J, Chang BH, Kurre P (2015) Serum exosome microRNA as a minimally-invasive early biomarker of AML. Sci Rep 5:11295
3. Paietta E Minimal residual disease in acute myeloid leukemia: coming of age. Hematol Am Soc Hematol Educ Program 2012, 2012: 35–42
4. Grove CS, Vassiliou GS (2014) Acute myeloid leukaemia: a paradigm for the clonal evolution of cancer? Dis Model Mech 7:941–951
5. Boyiadzis M, Whiteside TL (2016) Plasma-derived exosomes in acute myeloid leukemia for detection of minimal residual disease: are we ready? Expert Rev Mol Diagn 16:623–629
6. Becker A, Thakur BK, Weiss JM, Kim HS, Peinado H, Lyden D (2016) Extracellular vesicles in cancer: cell-to-cell mediators of metastasis. Cancer Cell 30:836–848
7. Keller S, Ridinger J, Rupp AK, Janssen JW, Altevogt P (2011) Body fluid derived exosomes as a novel template for clinical diagnostics. J Transl Med 9:86
8. Gould SJ, and Raposo G (2013) As we wait: coping with an imperfect nomenclature for extracellular vesicles, J Extracell Vesicles 2:20389
9. Raposo G, Stoorvogel W (2013) Extracellular vesicles: exosomes, microvesicles, and friends. J Cell Biol 200:373–383
10. Abels ER, Breakefield XO (2016) Introduction to extracellular vesicles: biogenesis, RNA cargo selection, content, release, and uptake. Cell Mol Neurobiol 36:301–312
11. Thakur BK, Zhang H, Becker A, Matei I, Huang Y, Costa-Silva B, Zheng Y, Hoshino A, Brazier H, Xiang J, Williams C, Rodriguez-Barrueco R, Silva JM, Zhang W, Hearn S, Elemento O, Paknejad N, Manova-Todorova K, Welte K, Bromberg J, Peinado H, Lyden D (2014) Double-stranded DNA in exosomes: a novel biomarker in cancer detection. Cell Res 24:766–769
12. Peinado H, Aleckovic M, Lavotshkin S, Matei I, Costa-Silva B, Moreno-Bueno G, Hergueta-Redondo M, Williams C, Garcia-Santos G, Ghajar C, Nitadori-Hoshino A, Hoffman C, Badal K, Garcia BA, Callahan MK, Yuan J, Martins VR, Skog J, Kaplan RN, Brady MS, Wolchok JD, Chapman PB, Kang Y, Bromberg J, Lyden D (2012) Melanoma exosomes educate bone marrow progenitor cells toward a pro-metastatic phenotype through MET. Nat Med 18:883–891
13. Pando A, Reagan JL, Quesenberry P, Fast LD (2018) Extracellular vesicles in leukemia. Leuk Res 64:52–60
14. Szczepanski MJ, Szajnik M, Welsh A, Whiteside TL, Boyiadzis M (2011) Blast-derived microvesicles in sera from patients with acute myeloid leukemia suppress natural killer cell function via membrane-associated transforming growth factor-beta1. Haematologica 96:1302–1309
15. Caivano A, Laurenzana I, De Luca L, La Rocca F, Simeon V, Trino S, D'Auria F, Traficante A, Maietti M, Izzo T, D'Arena G, Mansueto G, Pietrantuono G, Laurenti L, Musto P, Del Vecchio L (2015) High serum levels of extracellular vesicles expressing malignancy-related markers are released in patients with various types of hematological neoplastic disorders. Tumour Biol 36: 9739–9752
16. Caivano A, La Rocca F, Simeon V, Girasole M, Dinarelli S, Laurenzana I, De Stradis A, De Luca L, Trino S, Traficante A, D'Arena G, Mansueto G, Villani O, Pietrantuono G, Laurenti L, Del Vecchio L, Musto P (2017) MicroRNA-155 in serum-derived extracellular vesicles as a potential biomarker for hematologic malignancies - a short report. Cell Oncol (Dordr) 40:97–103
17. Huan J, Hornick NI, Shurtleff MJ, Skinner AM, Goloviznina NA, Roberts CT Jr, Kurre P (2013) RNA trafficking by acute myelogenous leukemia exosomes. Cancer Res 73:918–929
18. Hong CS, Muller L, Whiteside TL, Boyiadzis M (2014) Plasma exosomes as markers of therapeutic response in patients with acute myeloid leukemia. Front Immunol 5:160